



Title	High-throughput deterministic plasma etching using array-type plasma generator system
Author(s)	Sano, Yasuhisa; Nishida, Ken; Asada, Ryohei et al.
Citation	Review of Scientific Instruments. 2021, 92(12), p. 125107
Version Type	VoR
URL	<a href="https://hdl.handle.net/11094/86961">https://hdl.handle.net/11094/86961</a>
rights	This article may be downloaded for personal use only. Any other use requires prior permission of the author and AIP Publishing. This article appeared in (citation of published article) and may be found at <a href="https://doi.org/10.1063/5.0071623">https://doi.org/10.1063/5.0071623</a> .
Note	

*The University of Osaka Institutional Knowledge Archive : OUKA*

<https://ir.library.osaka-u.ac.jp/>

The University of Osaka

# High-throughput deterministic plasma etching using array-type plasma generator system <sup>EP</sup>

Cite as: Rev. Sci. Instrum. **92**, 125107 (2021); <https://doi.org/10.1063/5.0071623>

Submitted: 15 September 2021 • Accepted: 30 November 2021 • Published Online: 16 December 2021

 Yasuhisa Sano, Ken Nishida, Ryohei Asada, et al.

## COLLECTIONS

 This paper was selected as an Editor's Pick



View Online



Export Citation



CrossMark

## ARTICLES YOU MAY BE INTERESTED IN

[Homemade-HEMT-based transimpedance amplifier for high-resolution shot-noise measurements](#)

Review of Scientific Instruments **92**, 124712 (2021); <https://doi.org/10.1063/5.0076196>

[TrapREMI: A reaction microscope inside an electrostatic ion beam trap](#)

Review of Scientific Instruments **92**, 123201 (2021); <https://doi.org/10.1063/5.0065454>

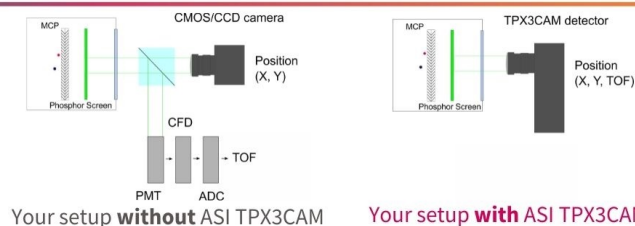
[Positron charge sensing using a double-gated graphene field effect transistor](#)

Review of Scientific Instruments **93**, 015002 (2022); <https://doi.org/10.1063/5.0069481>

[www.amscins.com](http://www.amscins.com)

 AMSTERDAM  
SCIENTIFIC  
INSTRUMENTS

**Simplify Your  
Set-up, Get  
Better Results!**



# High-throughput deterministic plasma etching using array-type plasma generator system

Cite as: Rev. Sci. Instrum. 92, 125107 (2021); doi: 10.1063/5.0071623

Submitted: 15 September 2021 • Accepted: 30 November 2021 •

Published Online: 16 December 2021



Yasuhisa Sano,<sup>1,a)</sup>  Ken Nishida,<sup>1</sup> Ryohei Asada,<sup>1</sup> Shinya Okayama,<sup>1</sup> Daisetsu Toh,<sup>1</sup>   
Satoshi Matsuyama,<sup>1,2</sup>  and Kazuto Yamauchi<sup>1,3</sup> 

## AFFILIATIONS

<sup>1</sup> Division of Precision Engineering and Applied Physics, Graduate School of Engineering, Osaka University, 2-1 Yamada-oka, Suita, Osaka 565-0871, Japan

<sup>2</sup> Department of Materials Physics, Graduate School of Engineering, Nagoya University, Furo-cho, Chikusa-ku, Nagoya, Aichi 464-8603, Japan

<sup>3</sup> Research Center for Precision Engineering, Graduate School of Engineering, Osaka University, 2-1 Yamada-oka, Suita, Osaka 565-0871, Japan

<sup>a)</sup> Author to whom correspondence should be addressed: sano@prec.eng.osaka-u.ac.jp

## ABSTRACT

A deterministic processing method is a high-precision finishing method, where the to-be-removed amount of material at each point of the work surface is calculated based on an accurately measured present surface shape and is removed precisely using a numerically controlled (NC) processing system. Although this method has achieved nanometer-scale accuracy, the method requires considerable time to scan the work surface, leading to low productivity. Therefore, using an individual on-off controllable array-type plasma generator covering the entire work surface, enabling simultaneous NC plasma processing is proposed herein. A novel intermittent gas flow system was constructed using cyclic on-off control of the gas supply and exhaust valves instead of the commonly used continuous gas flow to achieve uniform in-plane plasma etching. It was found that uniform removal could be achieved by combining it with a pulse-modulated high-frequency power supply and setting the plasma generation time in one cycle to be sufficiently short. Furthermore, a power control approach was developed for maintaining a constant plasma state, even while varying the plasma-generating array elements, which resulted in a demonstration experiment of NC plasma etching that successfully reduced the thickness variation of a silicon substrate.

Published under an exclusive license by AIP Publishing. <https://doi.org/10.1063/5.0071623>

## I. INTRODUCTION

Ultra-precise optics and substrates, such as perfectly flat mirrors, aspherical mirrors, aspherical lenses, large-diameter silicon wafers, crystal substrates for surface acoustic wave devices,<sup>1</sup> and photomask substrates for extreme-ultraviolet lithography,<sup>2</sup> require ultraprecision machining/finishing technology. These optics and substrates are critical for cutting-edge scientific instruments, such as high-brilliance beam lines,<sup>3</sup> gravitational wave telescopes,<sup>4</sup> and electronic device industries for information and communication technology (ICT). A precise global polishing procedure, such as chemical-mechanical planarization/polishing,<sup>5,6</sup> is used to attain the required accuracy, especially when the objective is a flat surface. When this method fails to achieve adequate accuracy or when the target shape is not flat, but spherical, aspherical, or free form,

deterministic processing methods are often used to reduce the figure error from the target shape.

The amount to be removed at each point of the work surface is calculated based on an accurately measured present surface shape and precisely removed using a numerically controlled (NC) processing system in a deterministic processing approach. Such a system has a processing head that removes a local area of the work surface and an NC x-y table for dwell time control of the processing head at each point on the surface. Several processing heads with completely different removal mechanisms have been reported, including NC elastic emission machining (EEM),<sup>7</sup> plasma-assisted chemical etching (PACE),<sup>8</sup> NC plasma chemical vaporization machining (PCVM),<sup>9-11</sup> magnetorheological finishing (MRF),<sup>12</sup> ion beam figuring (IBF),<sup>13</sup> plasma jet machining (PJM),<sup>14,15</sup> gas cluster ion beam (GCIB),<sup>16,17</sup> NC sacrificial oxidation,<sup>18</sup> and micro-electrolyte

jet machining.<sup>19</sup> Using these methods, nanometer-level accuracy has been achieved in fabricating high-precision x-ray mirrors,<sup>20</sup> ultra uniform 300-mm silicon-on-insulator substrates,<sup>21</sup> high-precision large-diameter aspherical lenses,<sup>22</sup> etc.

However, such conventional deterministic processing methods take a long time to scan the work surface, resulting in low productivity. Although this is a minor issue for master-craftsmanship-level special optics used in cutting-edge scientific instruments, it is fatal for the mass production of substrates, such as those for semiconductors and passive electronic devices. A deterministic processing method that can be applied to mass production is craved by industry. Therefore, we propose a novel deterministic processing method using an individually on-off controllable array-type plasma generator covering the entire work surface, enabling a simultaneous high-throughput NC process. With this method, NC processing can be done by directly controlling the exposure time in each area of the work surface instead of the dwell time control of a single localized plasma at each area of the work surface using a scanning x-y table with a programmed feed speed [Figs. 1(a) and 1(b)]. To realize such NC processing using an array-type plasma generator, it must have (1) an electrode structure that allows independent on-off control of the plasma of each electrode, regardless of the on-off status of neighboring electrodes and (2) the same plasma is generated at all electrodes, i.e., the gas composition in each plasma is the same.

First, to establish condition (1), the application to the NC sacrificial oxidation method, which automatically satisfies condition (2), was investigated. NC sacrificial oxidation is a precision-processing method for silicon, where the surface silicon to be removed is oxidized by an oxygen-containing plasma and then cleaned using hydrofluoric acid in a post-process, allowing subnanometer-level NC processing to be performed.<sup>18,21</sup> Although the oxidation reaction consumes the oxygen radicals generated in the plasma, the rate of oxygen concentration decrement is slow due to the relatively slow oxidation rate, which is only 1 nm/min. Additionally, since the reaction product is SiO<sub>2</sub>, no gas-phase reaction product is generated. Therefore, even if a gas flow in a constant direction parallel to the surface of the workpiece is applied, condition (2) is almost automatically satisfied. We have designed and fabricated an array-type electrode plasma generator, demonstrated that each electrode's plasma can be individually turned on and off regardless of the adjacent

electrodes' on-off status, and demonstrated highly efficient NC sacrificial oxidation processing.<sup>23,24</sup>

Thus, herein, we attempt to apply an array-type electrode plasma generator to PCVM, a plasma etching technique using a high-pressure plasma.<sup>9</sup> In PCVM, the gas composition in the plasma changes moment by moment due to the rapid consumption of reaction gases and the creation of gas-phase reaction products because of the high-speed plasma etching process. Therefore, condition (2) is not satisfied by simple gas flow in a constant direction parallel to the workpiece surface. In this paper, we propose a novel intermittent gas flow system using cyclic on-off control of the gas supply and exhaust valves instead of the commonly used continuous gas flow. Furthermore, this study investigates the processing conditions to satisfy condition (2) and demonstrates the high-throughput deterministic plasma etching. Realizing NC PCVM with an array-type plasma generator, the accuracy improvement of various mass production substrates is expected, such as synthetic quartz, quartz crystal, and semiconductor materials, which leads to higher performance of the devices and contributes to the ICT industry.

## II. EXPERIMENTAL APPARATUS

An array-type plasma generator is a type of parallel-plate-type plasma generator. It generates plasma between the high-frequency power-supplied electrodes and the parallel grounded work surface by a strong electric field. The distance between the electrode and work surfaces is approximately in the submillimeter to the several-millimeter range. Herein, the process gas was supplied to this thin space in the NC sacrificial oxidation experiments and it flowed in one direction. As mentioned before, this continuous unidirectional gas flow method can be used in cases where the gas composition change in the plasma is negligibly small. However, it causes nonuniform processing along the flow direction when a high consumption of the reactive gas or mass generation of the reaction gas product occurs. Therefore, it was conceived that to uniformly process the entire work surface using an array-type plasma generator, the gas flow should be stopped during plasma generation, and instead of the commonly used continuous gas flow systems, an intermittent gas flow system with cyclic on-off control of the gas supply and exhaust valves would be more effective, as follows:

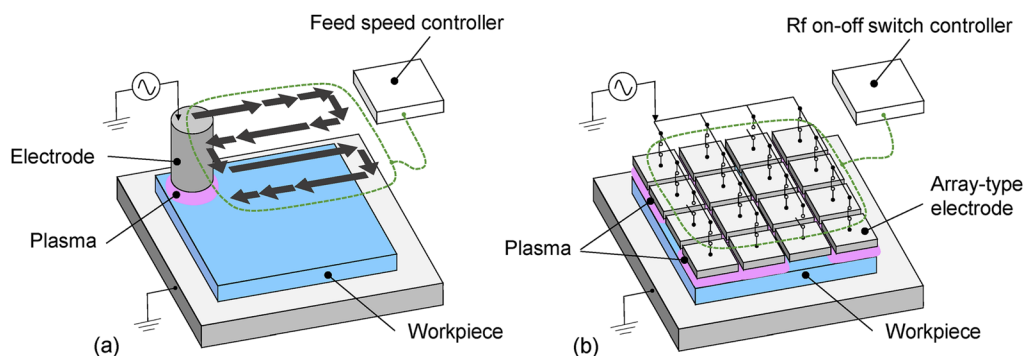


**FIG. 1.** Schematics of (a) conventional raster-scan-type NC plasma processing and (b) proposed simultaneous NC plasma processing using an array-type plasma generator (example of  $4 \times 4$  electrodes).

- (1) rapid vacuum evacuation,
- (2) supplying process gas instantaneously to the operating pressure, and
- (3) short-time plasma etching without any gas flow.

A prototype system was constructed using the above concept (Fig. 2). A vacuum buffer with greater volume than the plasma generation space was installed between the gas exhaust magnetic valve and the vacuum pump for rapid vacuum evacuation. A process gas tank, where a predetermined concentration of  $\text{SF}_6$  gas was diluted with He gas, was connected to the plasma generator through the gas supply magnetic valve and a vacuum regulator. The operating pressure was determined by the opening time of the gas supply valve after vacuum evacuation. Both the gas supply and exhaust valves were connected to the signal generator to control the opening time of both valves and their timings.

The matrix size of the array-type electrode is  $7 \times 7$ , and the electrode is square-shaped with 4.8-mm sides. The period of the electrodes is 5.0 mm, and the gap between the adjoining electrodes is 0.2 mm. A thin sapphire plate was placed on the array-type electrode's surface to avoid corrosion by fluorine radicals and unexpected arc discharge. Each electrode had its own electric switch for the plasma on-off control, connected to a PC. A 13.56-MHz radio frequency (RF) power supply that could be operated by a pulse modulation from an external pulse input was connected to the array-type electrodes through an impedance-matching unit for plasma generation. The RF-on time (pulse length) and its timing were also controlled by the signal generator, which controlled the gas supply and exhaust valves.

After wet cleaning with a sulfuric acid and hydrogen peroxide mixture, a commercially available silicon wafer was used as the sample. After the experiment, the sample's surface was measured using an interference microscope with a stitching feature. The removal profile was obtained by comparing the processed and preprocessed profiles. Atomic force microscopy was used to measure the surface roughness, and the root mean square (rms) roughness value in a  $2 \times 2 \mu\text{m}^2$  area was used for evaluating the roughness.

### III. EXPERIMENTAL RESULTS

#### A. Opening time of gas exhaust/supply magnetic valves

Figure 3 shows the relationship between the pressure in the array-type plasma generator and the opening time of the gas exhaust valve. After the gas exhaust valve is opened, the pressure decreases from the initial atmospheric pressure and reaches the lower detection limit (0.5 kPa) of the sensor pressure after 90 ms. Based on this, the opening time of the exhaust valve was set as 100 ms. Figure 4 shows the relationship between the pressure and the opening time of the gas supply valve. It was found that the pressure gradually increased with increasing opening time of the valve and that the operating pressure could be controlled by controlling the opening time of the gas supply valve. Although some variations exist in the pressure data, the standard deviation is  $\sim 0.1$  kPa, which could be negligible during such a repeating process. In the following experiments, the opening time of the gas supply valve was determined

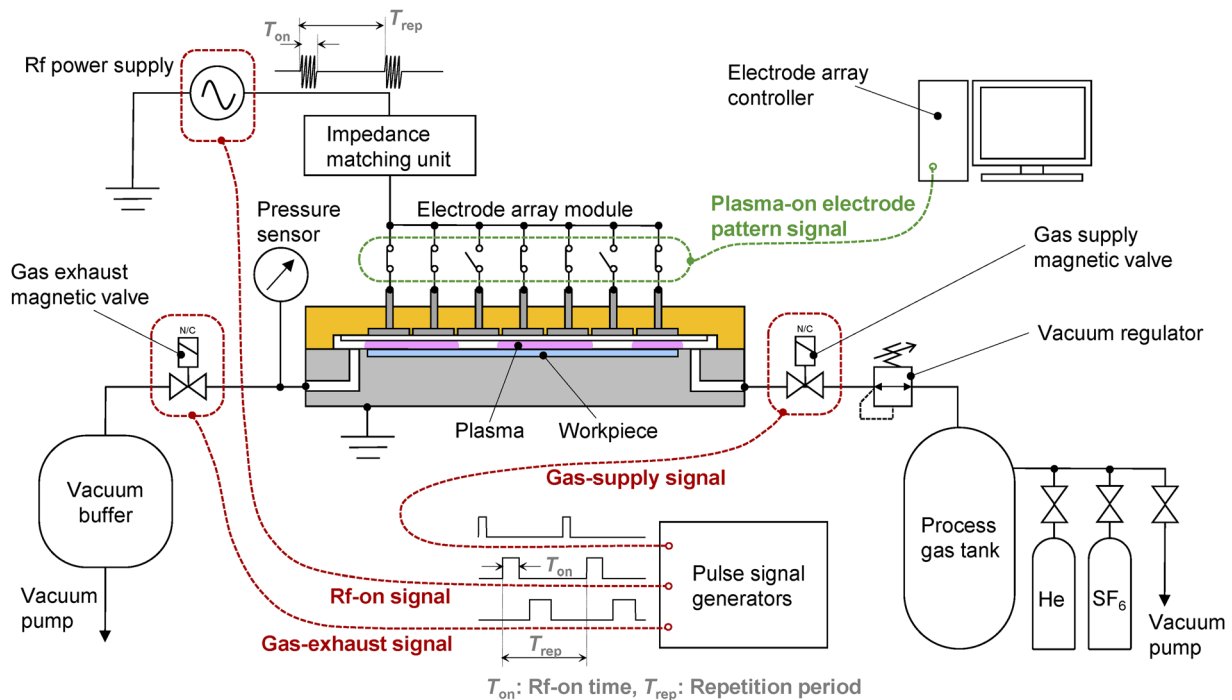


**FIG. 2.** Schematic of the NC plasma etching system using an array-type plasma generator. The system has pulse signal generators to control the opening time of the gas exhaust valve, opening time of the gas supply valve, and RF-on time for plasma generation.

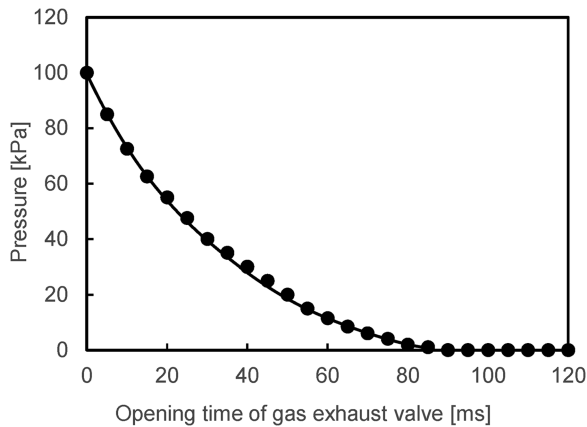


FIG. 3. Pressure-decreasing characteristics with the opening time of the gas exhaust valve.

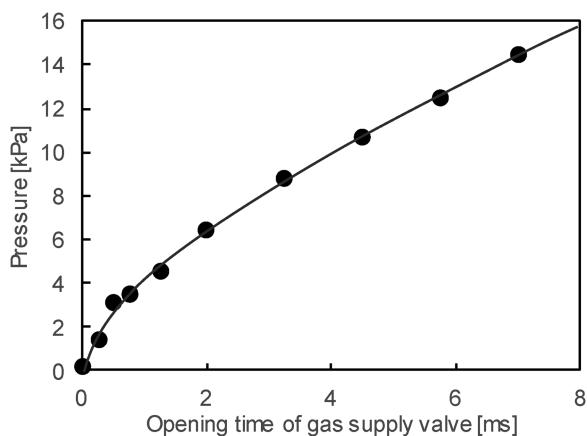


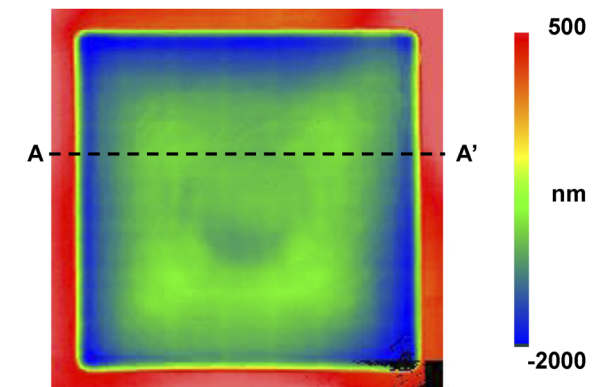
FIG. 4. Pressure-increasing characteristics with the opening time of the gas supply valve.

using Fig. 4 so that the chamber pressure would be the value as in the experimental conditions.

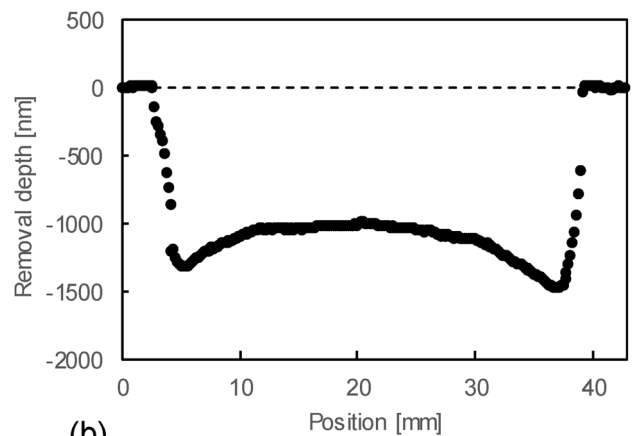
### B. RF-on time per cycle

The effects of the plasma-on time per cycle ( $T_{\text{on}}$  in Fig. 2) on the removed profiles were investigated using all 49 electrodes ( $7 \times 7$ ). As aforementioned, the opening times of the gas exhaust valve were set to 100 ms, whereas that of the gas supply valve was set to 2 ms corresponding to the operating pressure of 6 kPa. The repetition period ( $T_{\text{rep}}$  in Fig. 2) was set to 500 ms, and the RF-on times per cycle were 5, 20, 40, 50, 100, and 200 ms. Ten percent  $\text{SF}_6$  gas diluted with He gas was used as a process gas, and the peak power of the RF-power supply was 350 W. The total processing time was 5 min, i.e., 600 cycles.

Figure 5(a) shows an example of a surface profile obtained after the experiment, whereas Fig. 5(b) shows the A–A' line profile of Fig. 5(a). Figure 5(b) shows that the removal depth is nonuniform, i.e., the removal depth of the edge parts exceeds that of the center



(a) 10 mm

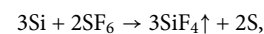


(b)

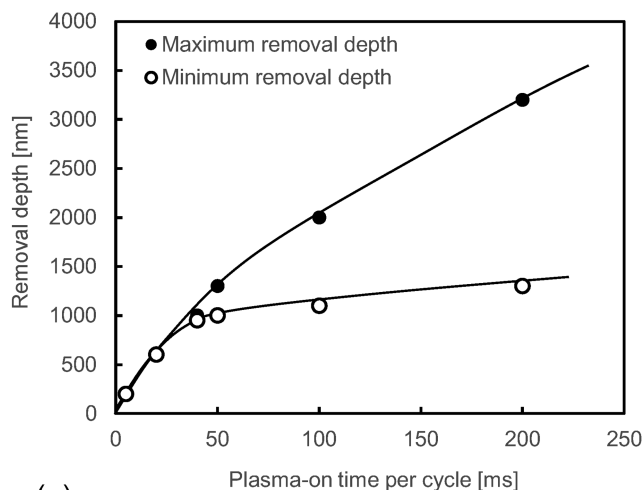
FIG. 5. Surface profile after experiment with the plasma-on time per cycle of 50 ms. (a) 2D profile and (b) A–A' line profile of (a) indicate nonuniform processing profiles, i.e., removal depth of the edge part exceeds that of the center part.

part. Therefore, the removal depths of the edge (maximum removal depth) and center (minimum removal depth) parts are plotted in Fig. 6(a) as a function of the RF-on time per cycle. Figure 6(a) shows that the removal depth of the edge part increases as the plasma-on time increases, whereas that of the center part is saturated at  $\sim 1000$  nm for RF-on times longer than 40 ms.

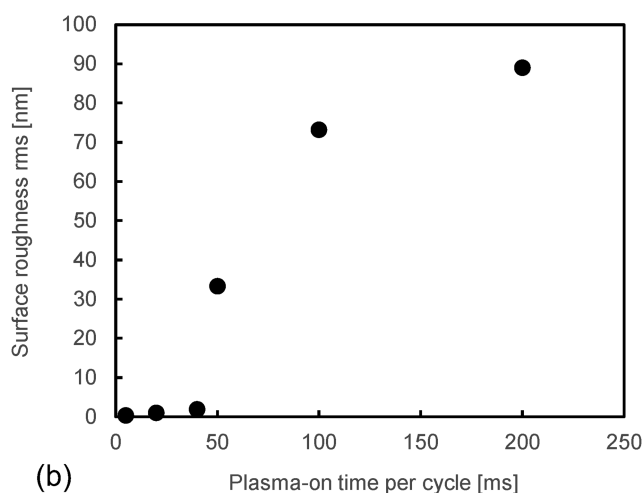
Because this 1000 nm is the result of the 600-cycle etching, the etching depth per cycle was determined to be 1.67 nm, i.e., the number of removed Si atoms per cycle was calculated to be  $1.7 \times 10^{-7}$  mol (the removal area is estimated to be  $1.2 \times 10^3 \text{ mm}^2$ ). However, given that the thickness of the plasma generation space (i.e., the gap between the electrode and work surfaces) is 1.5 mm, the number of  $\text{SF}_6$  gas molecules before plasma generation was calculated to be  $4.9 \times 10^{-7}$  mol. Assuming that the following chemical reaction occurs:



the number of  $\text{SiF}_4$  gas molecules (reaction gas product) can be determined to be  $1.7 \times 10^{-7}$  mol, indicating that the number of  $\text{SF}_6$



(a)



(b)

**FIG. 6.** (a) Removal depth and (b) surface roughness dependence on the plasma-on time per cycle. Filled and open circles indicate removal depths of edge (maximum removal depth) and center (minimum removal depth) parts. Surface roughness was measured at the center part of each sample.

gas molecules was reduced to  $3.8 \times 10^{-7}$  mol. Thus, here, the number of  $\text{SiF}_4$  gas molecules is almost half the number of  $\text{SF}_6$  gas molecules in the plasma.

From the above, it can be suggested that the saturation phenomenon of the removal depth at the center part is due to excess reaction products in the plasma. Figure 6(b) shows the measurement results of the surface roughness of the center part of each sample. A significant increase in the rms value was observed in the plasma-on time of 50 ms or more, corresponding to the saturation of the removal depth in the center part. When such a sample surface was observed by scanning electron microscopy (SEM), many particle-like convex shapes were observed. It was also confirmed by visual inspection that the surface became cloudy. Although a possibility exists that sulfur particles may generate and deposit on the

Time [min]	0-2	2-4	4-6
Number of ON-state electrodes	25	9	1
ON-electrode pattern			
Output rf peak power [W]	300	170	120

**FIG. 7.** Experimental conditions of plasma-on electrode variation with processing time.

surface, no sulfur detection was observed by the surface elemental analysis using an energy-dispersive x-ray spectroscope attached to the SEM. These results indicate that Si particles were regenerated in the plasma due to the increase in  $\text{SiF}_4$  gas molecules and redeposited on the processed surface, resulting in the removal depth saturation at the center part. Furthermore, another experimental result shows that under conditions where the plasma-on time is short enough, the surface roughness does not deteriorate, even when the number of cycles is increased.

The lack of saturation near the edge is thought to be due to more  $\text{SF}_6$  gas coming in from outside the plasma area and  $\text{SiF}_4$  gas being ejected outside the plasma due to a diffusion phenomenon. The asymmetric removal profile shown in Fig. 5 can be attributed to the diffusion phenomenon unevenness caused by the turbulence generated by the instantaneous introduction of gas in the gas supply process. In any case, in those plasma generation conditions, it was discovered that by maintaining the plasma-on time for each cycle below 40 ms, the uniform etching depth corresponding to condition (2) specified in the Introduction section could be obtained. This 40-ms threshold value depends on the processing parameters, such as the processing pressure and the gap between the electrode

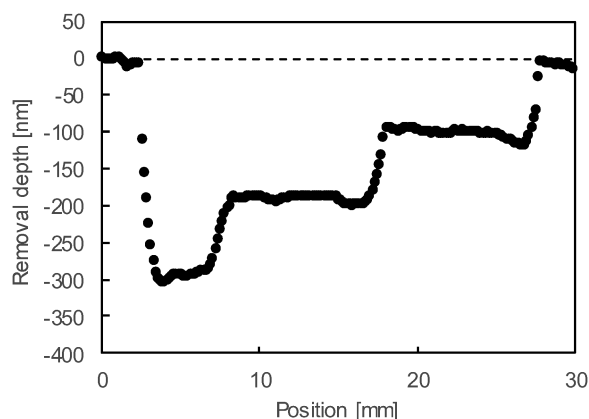


**FIG. 8.** Stair-like line profile of surface after experiment of varying the number of plasma-on electrodes.

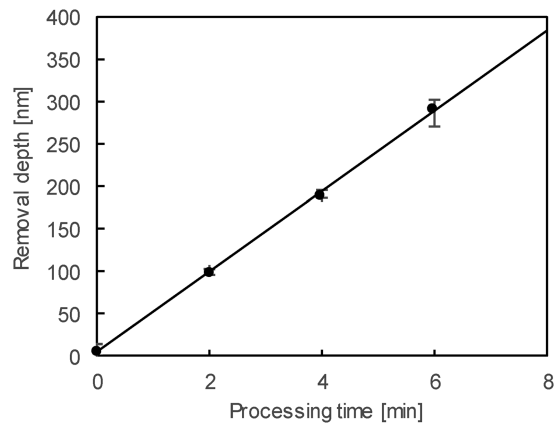


**FIG. 9.** Relationship between the processing time and removal depth shown in Fig. 8.

and work surfaces. An increase in these parameters increases the number of gas molecules between the electrode and work surfaces, which decreases the concentration of the reaction products, and thus increases the threshold plasma-on time. However, it will require more RF power.

### C. RF-power control

In the NC operation using the array-type plasma generator, the processing time of each electrode was programmed and controlled using a PC, indicating that the amount of plasma varied continuously during NC processing, and the supplied RF power should be controlled accordingly to maintain a consistent etching rate. Keeping the electrode voltage constant is critical because the plasma state depends on the electric field intensity between the electrode and work surfaces. Therefore, modifying the output power of the RF-power supply was proposed to achieve this requirement. A basic experiment was performed by changing the number of

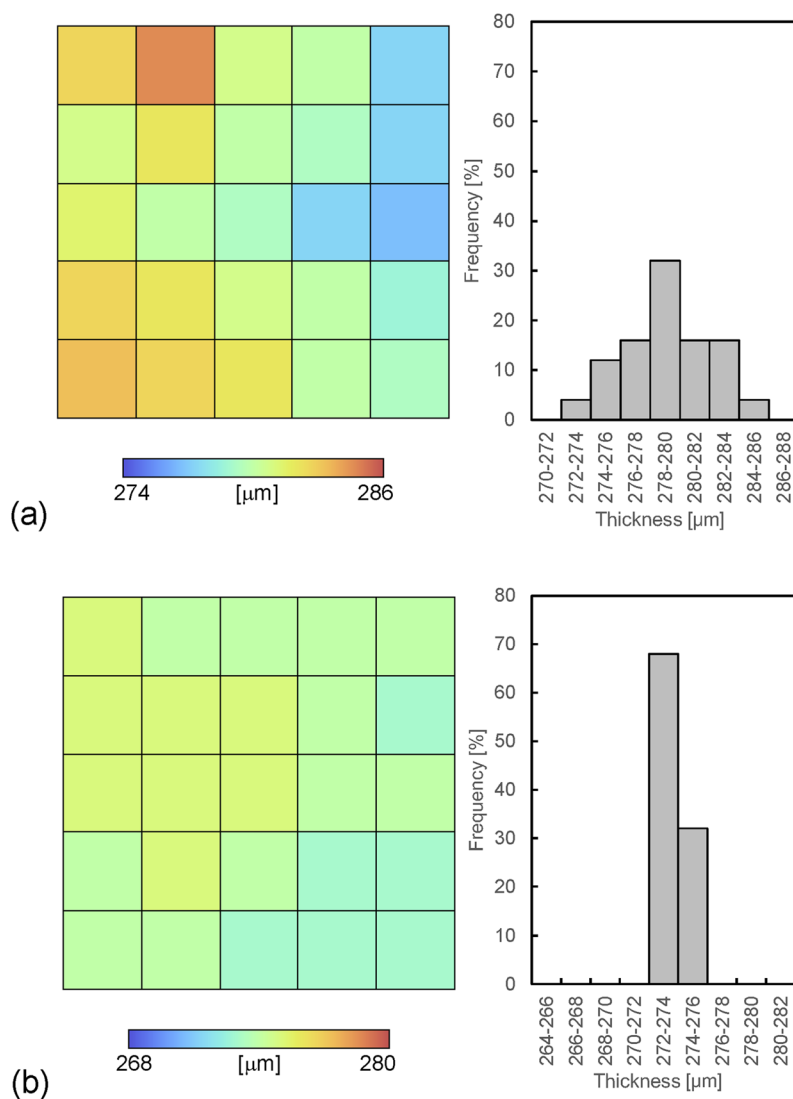


**FIG. 10.** Thickness profile of the Si substrate (a) before and (b) after 12-min NC plasma etching using an array-type plasma generator.

plasma-on electrodes under the conditions (Fig. 7). The number of electrodes in the on-state was set to 25, 9, and 1 in the first 2 min, the next 2 min, and the last 2 min, respectively. Other experimental parameters were the cycle length of 500 ms, RF-on time per cycle of 10 ms, He-to-SF<sub>6</sub> ratio of 9:1, and operating pressure of 10 kPa. The electrode voltage was monitored using an RF digital oscilloscope, and the RF output power decreased while decreasing the number of plasma-on electrodes to keep the peak voltage amplitude at 280 V. Consequently, it was kept constant at 280 V by controlling the RF output peak power (Fig. 7). A line profile of the removal depth after the experiment, corresponding to the five bottom electrodes in Fig. 7, is shown in Fig. 8. The removal depths for each processing time (2, 4, and 6 min) were read out from Fig. 8 and are plotted as a function of the processing time in Fig. 9. Despite the changing number of plasma-generating electrodes, it was shown that the removal depth was highly proportional to the processing time, demonstrating that the proposed control method for the RF output peak power operated excellently.

#### D. Demonstration of NC operation

To demonstrate deterministic processing using an array-type plasma generator, an experiment on the thickness uniformization of a silicon wafer was performed. Although the removal rate in Sec. III C was ~50 nm/min (Fig. 9) because the removal rate is almost proportional to  $T_{\text{on}}$  and inversely proportional to  $T_{\text{rep}}$ , which is the repetition frequency reciprocal, it can easily be increased by changing these parameters. In the NC machining experiments, the processing parameters were set such that the removal rate was ~1  $\mu\text{m}/\text{min}$ . The processing area was set as the center of a 25-mm-square area of a 2-in. silicon wafer. Figure 10(a) shows the initial thickness distribution of the sample measured by a digital thickness gauge. The plasma-on time of each electrode was set such that the thickness of the facing part was reduced to that of the thinnest part. Figure 10(b) shows the thickness distribution after the NC processing. After only 12-min processing, the 12- $\mu\text{m}$  thickness variation was successfully improved to 2  $\mu\text{m}$ . In this experiment, the power control to keep the electric voltage constant was done manually. The processing accuracy can be improved in the future by automating the power control. Note that we could create an area whose removal depth was zero. In the case of conventional raster-scan-type deterministic processing, the minimum removal volume depends on the maximum feed speed of the work table and is nonzero. Therefore, this method can be more effective for precise thickness control than conventional deterministic processing methods.

#### IV. SUMMARY

Instead of the typically used continuous gas flow systems, an array-type plasma generator for NC PCVM is presented herein, which uses an intermittent gas flow system with the cyclic on-off control of the gas supply and exhaust valves. Rapid deterministic processing was demonstrated by maintaining the plasma generation time in one cycle short and managing the RF peak power to keep the peak voltage amplitude of the electrode constant, even when the number of plasma-generating array elements changed.

Although the apparatus used herein could not treat a large area, there is theoretically no limitation on the processing area with this method because there is no continuous gas flow use. An array-type plasma generator for processing larger areas could be realized as long as a RF-power supply with higher power output and plasma on-off switch controller for larger numbers of electrodes are prepared. Because the lateral spatial resolution of this method depends on the size of each electrode element that constitutes the array-type plasma generator, it is necessary to use electrodes smaller than the spatial wavelength of the shape error to be corrected. Reducing the size of the electrode elements, including their on-off switch, is a challenge for the near future.

NC PCVM using an array-type plasma generator system enables deterministic processing with much higher throughput than conventional deterministic processing methods using a raster-scan system. This advantage is expected to cause a paradigm shift in high-precision-processing technology and make an essential contribution to industries producing precise substrates, such as those for semiconductors, passive electronic parts, and photomasks.

#### ACKNOWLEDGMENTS

This study was partially supported by the Adaptable and Seamless Technology Transfer Program through Target-driven R&D (A-STEP) from Japan Science and Technology Agency, Grant No. AS262Z01712K.

#### AUTHOR DECLARATIONS

##### Conflict of Interest

The authors have no conflicts to disclose.

#### DATA AVAILABILITY

The data that support the findings of this study are available from the corresponding author upon reasonable request.

#### REFERENCES

- 1C. C. W. Ruppel, *IEEE Trans. Ultrason., Ferroelectr., Freq. Control* **64**, 1390–1400 (2017).
- 2T. Shoki, M. Mitsui, M. Sakamoto, N. Sakaya, M. Ootsuka, T. Asakawa, T. Yamada, and H. Mitsui, *Proc. SPIE* **7636**, 76360U (2010).
- 3M. Yabashi and H. Tanaka, *Nat. Phys.* **11**, 12–14 (2017).
- 4K. Somiya, E. Hirose, and Y. Michimura, *Phys. Rev. D* **100**, 082005 (2019).
- 5M. Krishnan, J. W. Nalaskowski, and L. M. Cook, *Chem. Rev.* **110**, 178–204 (2010).
- 6H. Aida, T. Doi, H. Takeda, H. Katakura, S.-W. Kim, K. Koyama, T. Yamazaki, and M. Uneda, *Curr. Appl. Phys.* **12**, S41–S46 (2012).
- 7Y. Mori, K. Yamauchi, and K. Endo, *Precis. Eng.* **9**, 123–128 (1987).
- 8L. D. Bollinger, G. M. Gallatin, J. Samuels, G. Steinberg, and C. B. Zarowin, *Proc. SPIE* **1333**, 44 (1990).
- 9Y. Mori, K. Yamauchi, K. Yamamura, and Y. Sano, *Rev. Sci. Instrum.* **71**, 4627 (2000).
- 10Y. Mori, K. Yamamura, and Y. Sano, *Rev. Sci. Instrum.* **71**, 4620 (2000).
- 11Y. Sano, K. Yamamura, H. Mimura, K. Yamauchi, and Y. Mori, *Rev. Sci. Instrum.* **78**, 086102 (2007).

- <sup>12</sup>C. Maloney, J. P. Lormeau, and P. Dumas, *Proc. SPIE* **10009**, 100090R (2016).
- <sup>13</sup>T. Franz and T. Hänsel, *Proc. SPIE* **7655**, 765513 (2010).
- <sup>14</sup>T. Arnold, G. Böhm, and H. Paetzelt, *Contrib. Plasma Phys.* **54**, 145–154 (2014).
- <sup>15</sup>J. Meister and T. Arnold, *Plasma Chem. Plasma Process.* **31**, 91–107 (2011).
- <sup>16</sup>I. Yamada, J. Matsuo, N. Toyoda, and A. Kirkpatrick, *Mater. Sci. Eng.: R* **34**, 231–295 (2001).
- <sup>17</sup>J. O. Chu, L. P. Allen, W. Skinner, J. Hautala, T. G. Tetreault, R. MacCrimmon, C. Santeufemio, E. Degenkolb, and D. B. Fenner, in *2003 IEEE International Conference on SOI* (IEEE, 2003), pp. 46–47.
- <sup>18</sup>Y. Sano, T. Masuda, H. Mimura, and K. Yamauchi, *J. Cryst. Growth* **310**, 2173–2177 (2008).
- <sup>19</sup>W. Natsu, S. Ooshiro, and M. Kunieda, *CIRP J. Manuf. Sci. Technol.* **1**, 27–34 (2008).
- <sup>20</sup>S. Matsuyama, N. Kidani, H. Mimura, J. Kim, Y. Sano, K. Tamasaku, Y. Kohmura, M. Yabashi, T. Ishikawa, and K. Yamauchi, *Proc. SPIE* **8139**, 813905 (2011).
- <sup>21</sup>Y. Sano, T. Masuda, S. Kamisaka, H. Mimura, S. Matsuyama, and K. Yamauchi, in *IEEE International SOI Conference* (IEEE, 2008), pp. 165–166.
- <sup>22</sup>H. Takino, N. Shibata, H. Itoh, T. Kobayashi, K. Yamamura, Y. Sano, and Y. Mori, *Appl. Opt.* **41**, 3971–3977 (2002).
- <sup>23</sup>H. Takei, K. Yoshinaga, K. Matsuyama, S. Yamauchi, and Y. Sano, *Jpn. J. Appl. Phys., Part 1* **54**, 01AE03 (2015).
- <sup>24</sup>H. Takei, S. Kurio, S. Matsuyama, K. Yamauchi, and Y. Sano, *Rev. Sci. Instrum.* **87**, 105121 (2016).